

Molecular Dynamics Study of Orientational Cooperativity in Water

Pradeep Kumar,¹ Giancarlo Franzese,² Sergey V. Buldyrev,^{1,3} and H. Eugene Stanley¹

¹*Center for Polymer Studies and Department of Physics*

Boston University, Boston, MA 02215 USA

²*Departament de Física Fonamental, Universitat de Barcelona,*

Diagonal 647, Barcelona 08028, Spain

³*Department of Physics, Yeshiva University*

500 West 185th Street, New York, NY 10033 USA

(Dated: kfbs.tex 21 October 2005)

Abstract

Recent experiments on liquid water show collective dipole orientation fluctuations dramatically slower than expected (with relaxation time > 50 ns) [D. P. Shelton, Phys. Rev. B **72**, 020201(R) (2005)]. Molecular dynamics simulations of SPC/E water show large vortex-like structure of dipole field at ambient conditions surviving over 300 ps [J. Higo et al. PNAS, **98** 5961 (2001)]. Both results disagree with previous results on water dipoles in similar conditions, for which autocorrelation times are a few ps. Motivated by these recent results, we study the water dipole reorientation using molecular dynamics simulations in bulk SPC/E water for temperatures ranging from ambient 300 K down to the deep supercooled region of the phase diagram at 210 K. First, we calculate the dipole autocorrelation function and find that our simulations are well-described by a stretched exponential decay, from which we calculate the *orientational autocorrelation time* τ_a . Second, we define a second characteristic time, namely the time required for the randomization of molecular dipole orientation, the *self-dipole randomization time* τ_r , which is an upper limit on τ_a ; we find that $\tau_r \approx 5\tau_a$. Third, to check if there are correlated domains of dipoles in water which have large relaxation times compared to the individual dipoles, we calculate the randomization time τ_{box} of the site-dipole field, the net dipole moment formed by a set of molecules belonging to a box of edge L_{box} . We find that the *site-dipole randomization time* $\tau_{\text{box}} \approx 2.5\tau_a$ for $L_{\text{box}} \approx 3\text{\AA}$, i.e. it is shorter than the same quantity calculated for the self-dipole. Finally, we find that the orientational correlation length is short even at low T .

PACS numbers:

I. INTRODUCTION

Cooperative motion of water molecules [1] has been widely investigated in recent years, both by experiments [2, 3, 4, 5, 6, 7, 8, 9, 10, 11, 12, 13, 14, 15, 16, 17, 18, 19, 20, 21] and using molecular dynamics (MD) simulations [22, 23, 24, 25, 26, 27, 28, 29, 30, 31, 32, 33, 34, 35]. When water is cooled, the cooperativity of water molecules increases. Recent experiments on water show large correlated domains of dipoles at ambient conditions which have a relaxation time much larger than the autocorrelation time of individual dipoles [21]. MD studies of water models also show the possibility of formation of large correlated domains of dipoles in bulk as well as interfacial water [35] (where these correlated patterns of dipoles are pinned to solvated amino acids). These two studies are the principal motivation for the present investigation of the rotational cooperativity of water molecules.

A challenging problem is to develop methods of describing molecular motion in water that are better able to interpret experimental results, such as incoherent quasielastic neutron scattering, light scattering, dielectric, and nuclear magnetic resonance experiments [2, 18]. Several approximation proposals have been made for various autocorrelation functions describing both rotational and translational motion [20, 27]. These methods usually assume the Kohlrausch-Williams-Watts stretched exponential for the long time relaxation behavior of autocorrelation functions $\phi(t)$, as predicted by mode coupling theory (MCT),

$$\phi(t) = A \exp \left[- \left(\frac{t}{\tau_a} \right)^\beta \right]. \quad (1)$$

The relaxation time τ_a , the exponent β , and the non-ergodicity factor A are fitting parameters that depend on temperature T and density ρ [22, 23, 24, 25, 27, 28, 29, 30, 31].

Our interest here is to study the orientational dynamics of water by simulating SPC/E water. First we calculate the orientational autocorrelation time as the fitting parameter τ_a appearing in Eq. (1) [22, 23]. Other definitions are possible, e.g., based on other fitting functions for the orientational autocorrelation function decay, such as the biexponential [26, 36] or the von Schweidler law [33]. In all cases, the orientational autocorrelation times are the result of multi-parameter fitting procedures and roughly correspond to the characteristic time over which the orientational autocorrelation function decays by a factor of $e \approx 2.7$.

To find an upper limit of the orientational autocorrelation time τ_a , we will introduce a new quantity, the dipole randomization time τ_r , as the time after which the fluctuations of

the dipoles resemble an uncorrelated random variable [37] (Sec. IV A). We find $\tau_r > \tau_a$, and that τ_r and τ_a are linearly related (Sec. IV B), which is consistent with the MCT predictions that:

- (i) The autocorrelation times of all the autocorrelation functions of any fluctuation coupled to density fluctuations diverge at the same temperature T_{MCT} with the same power law exponent;
- (ii) All the characteristic times of a supercooled liquid are proportional to one another.

To characterize the increase of cooperativity and test for the presence of large correlated domains of dipoles, we also estimate the randomization time τ_{box} for the site-dipole field (Sec. V), a quantity which measures the relaxation of the net dipole moment of all the molecules inside a box of edge L_{box} . Our calculations show that τ_{box} when $L_{\text{box}} \approx 3\text{\AA}$ has a power law divergence at T_{MCT} , but with $\tau_{\text{box}} < \tau_r$. This result shows that the site-dipole field relaxes faster than the individual dipoles, resolving the apparent contradiction between Ref. [35] and previous results. Calculations of τ_{box} for larger boxes show that τ_{box} does not depend on the box size and hence do not support the experimental observation of long-lived large domains of correlated dipoles [21].

II. THE SPC/E MODEL

Our results are based on MD simulations of the extended simple point charge (SPC/E) model [38]. The distance between the oxygen atom and each of the hydrogen atoms is 0.1 nm, and the HOH angle is the tetrahedral angle 109.47° [39]. Each hydrogen atom has a charge $q_H = 0.432e$, where e is the electron charge, and the oxygen atom has a charge $q_O = -2q_H$. In addition, to model the van der Waals interaction, pairs of oxygen atoms of different molecules interact with a Lennard-Jones potential,

$$V_{i,j}(r_{i,j}) = 4\epsilon \left[\left(\frac{\sigma}{r_{i,j}} \right)^{12} - \left(\frac{\sigma}{r_{i,j}} \right)^6 \right], \quad (2)$$

where $r_{i,j}$ is the distance between molecules i and j , $\epsilon = 0.65$ kJ/mol and $\sigma = 0.3166$ nm.

We perform MD simulations for a system of $N = 1728$ molecules at density $\rho = 1.0$ g/cm³, $210 \text{ K} \leq T \leq 300 \text{ K}$, with periodic boundary conditions and a simulation time step of 1 fs. The temperature is controlled by the Berendsen method of rescaling the velocities [40]. The

long-range Coulombic interactions [41] are treated with the reaction field technique with a cutoff of 0.79 nm. For each state point, we run two independent simulations to improve statistics.

III. THE ORIENTATIONAL AUTOCORRELATION FUNCTION $C_1(t)$

To estimate the orientational autocorrelation time of water molecules in the supercooled regime, we average the scalar product of the normalized dipole vectors $\vec{\mu}_i$ of each water molecule i in the system,

$$\begin{aligned} C_1(t) &\equiv \left\langle \sum_{i=1}^N \vec{\mu}_i(t) \cdot \vec{\mu}_i(0) \right\rangle \\ &= \frac{1}{N} \sum_{i=1}^N \langle \cos \theta_i(t) \rangle, \end{aligned} \quad (3)$$

where $\theta_i(t)$ is the angle between $\vec{\mu}_i(t)$ and $\vec{\mu}_i(0)$. This function corresponds to the average of the Legendre polynomial $P_1(\cos \theta_i(t))$ evaluated for each molecule and can be directly measured by dielectric experiments.

Figure 1(a) plots $C_1(t)$ for $210 \text{ K} \leq T \leq 300 \text{ K}$, and displays the two-step decay of typical glass-forming systems. The long-time regime at low T can be fit well by Eq. (1) and the fitting parameters are shown in Table I. Both parameters in Eq. (1), A and β , show weak dependences on T . The resulting values of these parameters are consistent with previous simulations of a smaller system of SPC/E molecules [23].

The estimated autocorrelation times τ_a agree (Fig. 2) with the power law behavior predicted by the MCT,

$$\tau_a \sim (T - T_{\text{MCT}})^{-\gamma_a}. \quad (4)$$

We estimate $T_{\text{MCT}} = (194 \pm 4) \text{ K}$ and $\gamma_a = 2.9 \pm 0.3$, in agreement with previous results for similar densities and temperatures [24].

The estimated values of τ_a , verify well the the von Schweidler law (Appendix) and the *time-temperature superposition principle* predicted by MCT, i.e. that the autocorrelation functions in the α -relaxation regime at different temperatures follow the same master curve if the time is rescaled by the autocorrelation time (Fig. 1b) [29].

IV. THE SELF-DIPOLE RANDOMIZATION TIME τ_r

A. Definition and Methods

Here we define the randomization time τ_r , a new quantity that we propose to characterize the orientational autocorrelation time. We consider the normalized dipole $\vec{\mu}_i$ of molecule i over a time interval $\Delta t = \mathcal{N}\delta t$,

$$\bar{\mu}_i \equiv \frac{1}{\mathcal{N}} \sum_{k=0}^{\mathcal{N}} \vec{\mu}_i(t_k), \quad (5)$$

where $\bar{\mu}_i$ is a function of δt and Δt , $t_k \equiv k\delta t$, and δt is the time interval between two consecutive samples of $\vec{\mu}_i$.

If δt is greater than the autocorrelation time of $\vec{\mu}_i$, then two consecutive samples $\vec{\mu}_i(t)$ and $\vec{\mu}_i(t + \delta t)$ are *independent*, hence $\langle \vec{\mu}_i(t_j) \cdot \vec{\mu}_i(t_k) \rangle = 0$ if $j \neq k$, where $\langle \dots \rangle$ denotes the average over all the molecules N in the system. Hence

$$\langle \bar{\mu}_i^2 \rangle \equiv \langle \bar{\mu}_i \cdot \bar{\mu}_i \rangle \equiv \frac{1}{\mathcal{N}^2} \langle \sum_{j,k} \vec{\mu}_i(t_j) \cdot \vec{\mu}_i(t_k) \rangle = \frac{1}{\mathcal{N}}, \quad (6)$$

because $\langle (\vec{\mu}_i)^2 \rangle = 1$ for any t_k , and

$$\mu_{\text{rms}} \equiv \sqrt{\langle \bar{\mu}_i^2 \rangle} = \frac{1}{\sqrt{\mathcal{N}}} = \sqrt{\frac{\delta t}{\Delta t}}. \quad (7)$$

This is the result of a *freely jointed chain* of \mathcal{N} bonds of the same length, for which the mean square end-to-end distance is $\mathcal{N}^2 \langle \bar{\mu}_i^2 \rangle = \mathcal{N}$ [42]. Therefore, if δt is larger than the orientational autocorrelation time for $\vec{\mu}_i$, the μ_{rms} decreases as $1/\sqrt{\Delta t}$.

If, instead, δt is shorter than the orientational autocorrelation time, consecutive elements in the sum in Eq. (6) are correlated $\langle \vec{\mu}_i(t) \cdot \vec{\mu}_i(t + \delta t) \rangle = z$, resulting in a smaller fluctuation. This can be formally understood by considering the *freely rotating chain* model [42], where consecutive bonds in the chain are free to rotate, each around the axis of the previous bond, at an angle θ , such that $\cos(\theta) = z$. With this assumption, the resulting mean square end-to-end distance for n bonds of unit length is

$$\langle r_n^2 \rangle = n \frac{1+z}{1-z} - 2z \frac{1-z^n}{(1-z)^2}. \quad (8)$$

In the case of small θ , we have $z = 1 - \epsilon + O(\epsilon^2)$, with $\epsilon = \theta^2/2 \ll 1$ and $z^n \simeq \exp(-n\epsilon)$.

Then, from Eq. (8), we obtain

$$\left\langle \frac{1}{n} \sqrt{r_n^2} \right\rangle = \frac{1}{n\epsilon} [2(n\epsilon - 1 - e^{-n\epsilon})]^{1/2}. \quad (9)$$

In our problem, the bonds are dipole vectors sampled at time intervals δt , and $n = \Delta t/\delta t = \mathcal{N}$. Therefore Eq. (9) becomes

$$\mu_{\text{rms}} \sim \frac{1}{\mathcal{N}\epsilon} [2(\mathcal{N}\epsilon - 1 - e^{-\mathcal{N}\epsilon})]^{1/2}. \quad (10)$$

The right-hand side of this equation behaves as $1/\sqrt{\Delta t}$ for $\mathcal{N} \rightarrow \infty$, i.e., the random case behavior is recovered for large $\Delta t/\delta t$.

Therefore, if we define τ_r as the time at which the correlation goes to zero as $1/\sqrt{\Delta t}$, it is possible to see that

$$\mu_{\text{rms}} \sim 1/\sqrt{\Delta t} \begin{cases} \text{for any } \Delta t & \text{if } \delta t \geq \tau_r \\ \text{for } \Delta t \gg \tau_r & \text{if } \delta t < \tau_r. \end{cases} \quad (11)$$

If we consider the fluctuation of any observable, the relation (11) defines the randomization time τ_r for that observable [37] and τ_r is equal to the smallest δt such that $\mu_{\text{rms}} \sim 1/\sqrt{\Delta t}$ for any Δt .

B. Calculation of τ_r

In Fig. 3, we show μ_{rms} for $T = 220$ K calculated for different values of δt . For small δt and small Δt , μ_{rms} deviates largely from the asymptotic law. However, for increasing δt , the deviation decreases. For $\delta t = 1280$ ps the asymptotic behavior, within the error of our calculations, is reached.

The evaluation of τ_r from a plot such as in Fig. 3 could be problematic, since it depends critically on the data errors. Therefore, to define in a clear way τ_r , we fit the first eight points ($\Delta t = \delta t, 2\delta t, \dots, 8\delta t$) using

$$\mu_{\text{rms}} \sim (\Delta t)^\lambda, \quad (12)$$

where $\lambda = \lambda(\delta t)$. In this way we study how the deviation from the asymptotic regime decreases by increasing δt . We find that the exponent λ increases toward the asymptotic value $1/2$ for increasing δt , and $\lambda = 1/2$ for any $\delta t \geq \tau_r$ (Fig. 4). We therefore define τ_r as the extrapolated values of δt at which $\lambda = 1/2$. We find that λ approaches $1/2$ as $1/\delta t$, to the leading order, for low temperatures (Fig. 4).

The resulting values of τ_r are presented in Fig.5a as functions of $T - T_{\text{MCT}}$, showing that the power law behavior Eq. (4) is well satisfied by τ_r . In this case our estimates are

$T_{\text{MCT}} = (191.5 \pm 2.5)$ K and $\gamma_r = 3.3 \pm 0.2$, both consistent within the errors with the estimates based on τ_a (Fig.2). Therefore, the prediction (i) of MCT is verified.

By plotting τ_r against τ_a , we verify the MCT prediction (ii). We find (Fig. 6) that τ_r and τ_a are linearly related and that τ_r is approximately five times larger than τ_a .

The large value of τ_r with respect to τ_a is consistent with the fact that the latter measures the decay of the self-dipole correlation to a finite value, while the first measures the time needed for the self-dipole autocorrelation to decay to zero. This result is also reminiscent of the recent MD analysis in bulk water for the *site-dipole field*, a measure of the average orientation of the molecules passing through each spatial position, recently introduced in Ref. [35]. Higo et al. [35] find coherent patterns for the site-dipole field, at ambient pressure and $T = 298$ K and $T = 300$ K, that persist for more than 100 ps, a time much larger than the single molecule orientational relaxation time τ_a of approximately 5 ps (Table I). It is, therefore, interesting to calculate the randomization time τ_{box} and to find its relation with the autocorrelation time τ_a for $T \rightarrow T_{\text{MCT}}$.

V. THE SITE-DIPOLE FIELD

To check if there are large correlated domains of dipoles in water which have large relaxation times compared to the individual dipole correlation time, we next study site-dipole field introduced by Higo et. al. [35]. We define the instantaneous coarse-grained site-dipole field

$$\vec{d}_i^v \equiv \vec{d}(\vec{r}_i, t) \equiv \frac{1}{n_i(t)} \sum_{\text{box}} \vec{\mu}_i \quad (13)$$

as the average of dipoles $\vec{\mu}_i$ of all the molecules $n_i(t)$ at time t belonging to box i of edge L_{box} , volume $v = L_{\text{box}}^3$ and centered at \vec{r}_i . If $n_i(t) = 0$, then $\vec{d}_i^v = 0$ by definition [43, 44]. We chose vectors \vec{r}_i in such a way that the corresponding boxes do not overlap [45]. The time average \bar{d}_i^v over an interval Δt , is defined analogously to Eq. (5). The rms average d_{rms}^v , is defined in analogy to Eq. (6) and (7), but instead of summation over all molecules we perform a summation over all boxes.

Since the argument presented for μ_{rms} is also valid for d_{rms}^v , the relation (11) also holds for d_{rms}^v and allows us to estimate the randomization time τ_{box} for d_{rms}^v . We find that τ_{box} , calculated for $L_{\text{box}} = 3.33\text{\AA}$, diverges at $T_{\text{box}} = (194 \pm 2)$ K with a power law with exponent $\gamma_{\text{box}} = 3.2 \pm 0.2$, consistent with our estimates of γ_a and T_{MCT} , respectively (Fig. 7).

If we compare τ_{box} with τ_r (Fig. 8), we again find a linear relation, as in Fig. 6 for τ_a , consistent with the MCT statement (ii). The proportionality factor is approximately 2.5 [46], smaller than the factor ≈ 5 found for τ_r in Fig. 6. Therefore, we conclude that in bulk water the coarse-grained site-dipole randomization time τ_{box} is larger than the self-dipole autocorrelation time τ_a , but smaller than τ_r . Thus we do not find a significant increase in the box dipole autocorrelation time compared to the autocorrelation time τ_a . These results do not support the results of Refs. [21, 35].

To test the existence of cooperative domains in the SPC/E model, we perform coarse-graining of the dipole field for boxes of sizes $3.33 \text{ \AA} \leq L_{\text{box}} \leq 10 \text{ \AA}$. If the dipoles of molecules in the box are independent random variables, d_{rms}^v must be inversely proportional to $\sqrt{\langle n_i \rangle} \propto \sqrt{v}$, since the average number of molecules in the box is proportional to its volume. The dependence of $d_{\text{rms}}^v \sqrt{v}$ on time t must be the same for the boxes of different volumes v . We show in Fig. 9 the behavior of $d_{\text{rms}}^v \sqrt{v}$ for $T = 220 \text{ K}$ and $T = 300 \text{ K}$. The collapse of all the curves confirms the hypothesis of very weak autocorrelations among neighboring dipoles. Only for $T = 220 \text{ K}$ we observe a weak size dependence of $d_{\text{rms}}^v \sqrt{v}$ for the smallest size, suggesting that at this T the correlation length is between 3.33 and 6 \AA , comparable to the dipole-dipole correlation length at ambient T [44]. Thus our simulations support the existence of only short range orientational autocorrelation in SPC/E water even at low T .

VI. DISCUSSION

Considerable numerical evidence shows that MCT predictions apply to orientational dynamics of water, despite the fact that MCT has been developed for particles interacting through spherically symmetric potentials [47]. However, recent extensions of MCT to liquids of linear molecules [48, 49], and single solute molecules in a simple solvent liquid [50], confirm the main MCT predictions about the orientational autocorrelation functions [33].

Our study of supercooled water confirms the validity of MCT predictions for the orientational autocorrelation time τ_a , estimated through a stretched exponential of the dipole autocorrelation function, for the temperature range $210 \text{ K} \leq T \leq 300 \text{ K}$ at density $\rho = 1 \text{ g/cm}^3$. Our results agree with the time-temperature superposition principle and the power law Eq. (4), with $T_{\text{MCT}} = (194 \pm 4) \text{ K}$ and $\gamma_a = 2.9 \pm 0.3$.

By evaluating the randomization time τ_r , defined as the time needed to randomize the molecular dipoles, we verify the MCT prediction that all the characteristic times of quantities coupled to density fluctuations of a supercooled liquid are proportional to each other and follow the same power law Eq. (4). We find $\tau_r \approx 5 \tau_a$, with $T_{\text{MCT}} = (191.5 \pm 2.5)$ K and $\gamma_r = 3.3 \pm 0.2$, consistent with the estimates based on the calculation of τ_a .

We also calculate the randomization time τ_{box} for the box dipole field, a quantity introduced in Ref. [35] to measure the local orientational memory of molecules passing through a given spatial position. Our results for $L_{\text{box}} = 3.33 \text{ \AA}$ show that τ_{box} diverges at $T_{\text{box}} = T_{\text{MCT}}$, following a power law with exponent $\gamma_{\text{box}} = \gamma_a$, and that $\tau_{\text{box}} \approx \tau_r/2$. As a consequence, the local memory is lost faster than the self-dipole orientational memory.

Our results also show the existence of domains of correlated dipoles of short spatial range, with a correlation length comparable to the dipole-dipole correlation length at ambient T [44]. Whether this conclusion is specific to the SPC/E model with reaction field is an open question, and requires further investigation using other models of water, e.g. polarizable models.

Acknowledgments

We thank N. Giovambattista for his helpful collaboration on initial phase of this work. We thank the NSF Chemistry Program for support. GF thanks the Spanish Ministerio de Educación y Ciencia (Programa Ramón y Cajal and Grant No. FIS2004-03454), and M. Sasai for his hospitality during a visit to Nagoya University.

APPENDIX A: THE VON SCHWEIDLER LAW

The MCT predicts that the autocorrelation function departs from the plateau A as a power law with exponent b , known as the von Schweidler law,

$$C_1(t) - A \sim -(t/\tau_a)^b, \quad (\text{A1})$$

where the von Schweidler exponent b does not depend on T . We verify that at lower temperatures Eq. (A1) holds for roughly two decades in time (Fig. 10) and we find a clear deviation only for $T \geq 260$ K at short times, possibly due to the fact that for $T \geq 260$ K it

is more difficult to estimate the plateau A . The estimated value of b is 0.6 ± 0.1 , consistent with previous results [29] and with the MCT prediction that γ_a , a , and b are related by the equation

$$\gamma_a = \frac{1}{2a} + \frac{1}{2b}. \quad (\text{A2})$$

Here a is the exponent of the power law that describes the short-time approach to the plateau $C_1 - A \sim t^{-a}$, and a is related to b by the transcendental equation

$$\frac{[\Gamma(1-a)]^2}{\Gamma(1-2a)} = \frac{[\Gamma(1+b)]^2}{\Gamma(1+2b)}, \quad (\text{A3})$$

where $\Gamma(x)$ is the Euler gamma function. Our estimates of b and γ_a are consistent with both Eqs. (A2) and (A3) with $a = 0.25 \pm 0.05$.

The values of the exponents a , b and γ_a are not universal, but depend on density. However, the rescaling of the autocorrelation functions for different T on the same master curve, shows that the orientational correlation function depends on T and ρ only through the dependence on τ_a , as predicted by the MCT.

-
- [1] See, e.g., M.-C. Bellissent-Funel, ed., *Hydration Processes in Biology: Theoretical and Experimental Approaches* (IOS Press, Amsterdam, 1999); P. G. Debenedetti, J. Phys. Cond. Matt. **15**, R1669 (2003); P. G. Debenedetti and H. E. Stanley, Physics Today **56** [issue 6], 40–46 (2003); O. Mishima and H. E. Stanley, Nature **396**, 329–335 (1998).
 - [2] G. Sposito, J. Chem. Phys. **74**, 6943 (1981).
 - [3] S. H. Chen, J. Teixeira, and R. Nicklow, Phys. Rev. A **26**, 3477 (1982).
 - [4] F. X. Prielmeir, E. W. Lang, R. J. Speedy, and H. D. Lüdemann, Phys. Rev. Lett. **59**, 1128 (1987).
 - [5] C. A. Angell, Nature **331**, 206 (1988).
 - [6] V. Mazzacurati, A. Nucara, M. A. Ricci, G. Ruocco, and G. Signorelli, J. Chem. Phys. **93**, 7767 (1990).
 - [7] F. Sobron, F. Puebla, F. Rull, and O. F. Nielsen, Chem. Phys. Lett. **185**, 393 (1991).
 - [8] K. Mizoguchi, Y. Hori, and Y. Tominaga, J. Chem. Phys. **97**, 1961 (1992).
 - [9] S.-H. Chen, in *Hydrogen-Bonded Liquids*, Vol. 329 of NATO Advanced Studies Institute Series, edited by J. C. Dore and J. Teixeira (Kluwer Academic, Dordrecht, 1991), pp. 289–332; S.

- Dellerue and M.-C. Bellissent-Funel, *Chem. Phys.* **258**, 315 (2000); A. R. Bizzarri and S. Cannistraro, *J. Phys. Chem. B* **106**, 6617 (2002).
- [10] S.-H. Chen, P. Gallo, and M.-C. Bellissent Funel, *Can. J. Phys.* **73**, 703 (1995).
- [11] M.-C. Bellissent-Funel, S.-H. Chen, and J.-M. Zanotti, *Phys. Rev. E* **51**, 4558 (1995).
- [12] J.-M. Zanotti, M.-C. Bellissent-Funel, and S.-H. Chen, *Phys. Rev. E* **59**, 3084 (1999).
- [13] S. Takahara, M. Nakano, S. Kittaka, Y. Kuroda, T. Mori, H. Hamano, and T. Yamaguchi, *J. Phys. Chem.* **103**, 5814 (1999).
- [14] J. T. Cabral, A. Luzar, J. Teixeira, and M.-C. Bellissent-Funel, *J. Chem. Phys.* **113**, 8736 (2000).
- [15] V. Crupi, D. Majolino, P. Migliardo, and V. Venuti, *J. Phys. Chem. A* **104**, 11000 (2000).
- [16] V. Crupi, D. Majolino, P. Migliardo, and V. Venuti, *J. Chem. Phys. B* **106**, 10884 (2002).
- [17] S. Magazu and G. Maisano, *J. Mol. Liq.* **93**, 7 (2001).
- [18] Y. Xie, K. F. Ludwig, Jr., G. Morales, D. E. Hare, and C. M. Sorensen, *Phys. Rev. Lett.* **71**, 2050 (1993).
- [19] L. Bosio, J. Teixeira, and H. E. Stanley, *Phys. Rev. Lett.* **46**, 597 (1981).
- [20] J. Teixeira, M.-C. Bellissent-Funel, S.-H. Chen, and A. J. Dianoux, *Phys. Rev. A* **31**, 1913 (1985).
- [21] D. P. Shelton, *Phys. Rev. B*, **72**, 020201 (2005).
- [22] P. Gallo, F. Sciortino, P. Tartaglia, and S.-H. Chen, *Phys. Rev. Lett.* **76**, 2730 (1996).
- [23] F. Sciortino, P. Gallo, P. Tartaglia, and S.-H. Chen, *Phys. Rev. E* **54**, 6331 (1996).
- [24] F. W. Starr, S. Harrington, F. Sciortino, H. E. Stanley, *Phys. Rev. Lett.* **82**, 3629 (1999); F. W. Starr, F. Sciortino, and H. E. Stanley, *Phys. Rev. E* **60**, 6757 (1999).
- [25] D. Paschek and A. Geiger, *J. Phys. Chem. B* **103**, 4139 (1999); P. Gallo, M. Rovere, and E. Spohr, *Phys. Rev. Lett.* **85**, 4317 (2000).
- [26] P. A. Netz, F. W. Starr, H. E. Stanley, and M. C. Barbosa, *J. Chem. Phys.* **115**, 344 (2001); P. A. Netz, F. W. Starr, M. C. Barbosa, and H. E. Stanley, *J. Mol. Liq.* **101**, 159 (2002).
- [27] S.-H. Chen, C. Liao, F. Sciortino, P. Gallo, and P. Tartaglia, *Phys. Rev. E* **59**, 6708 (1999); C. Y. Liao, F. Sciortino, and S. H. Chen, *Phys. Rev. E* **60**, 6776 (1999).
- [28] D. Di Cola, A. Deriu, M. Sampoli, and A. Torcini, *J. Chem. Phys.* **104**, 4223 (1996); S.-H. Chen, P. Gallo, F. Sciortino, and P. Tartaglia, *Phys. Rev. E* **56**, 4231 (1997).
- [29] F. Sciortino, L. Fabbian, S. H. Chen, and P. Tartaglia, *Phys. Rev. E* **56**, 5397 (1997); L.

- Fabbian, F. Sciortino, and P. Tartaglia, *J. Non-Cryst. Solids* **235-237**, 350 (1998).
- [30] A. Faraone, L. Liu, C. Y. Mou, P. C. Shih, J. R. D. Copley, and S.-H. Chen, *J. Chem. Phys.* **119**, 3963 (2003).
- [31] L. Liu, A. Faraone, and S.-H. Chen, *Phys. Rev. E* **65**, 041506 (2002).
- [32] L. Fabbian, F. Sciortino, F. Thiery, and P. Tartaglia, *Phys. Rev. E* **57**, 1485 (1998); L. Fabbian, R. Schilling, F. Sciortino, P. Tartaglia, and C. Theis, *Phys. Rev. E* **58**, 7272 (1998); L. Fabbian, F. Sciortino, and P. Tartaglia, *Phil. Mag. B* **77**, 499 (1998).
- [33] L. Fabbian, A. Latz, R. Schilling, F. Sciortino, P. Tartaglia, and C. Theis, *Phys. Rev. E* **62**, 2388 (2000).
- [34] A. Faraone, L. Liu, and S.-H. Chen, *J. Chem. Phys.* **119**, 6302 (2003).
- [35] J. Higo, M. Sasai, H. Shirai, H. Nakamura, and T. Kugimiya, *Proc. Nat. Acad. Sci.* **98**, 5961 (2001).
- [36] Y.-L. Yhe and C.-Y. Mou, *J. Phys. Chem B* **103**, 3699 (1999).
- [37] See, e.g., K. Binder, ed., *Monte Carlo Methods in Statistical Physics* (Springer-Verlag, Berlin, 1979).
- [38] H. J. C. Berendsen, J. R. Grigera, and T. P. Stroatsma, *J. Phys. Chem.* **91**, 6269 (1987).
- [39] Microwave spectroscopy and infrared spectroscopy on H₂O at equilibrium in the gas phase give 0.9575Å for the O-H distance and 104.51° for the HOH angle [D. R. Lide *CRC Handbook of Chemistry and Physics, 84th Edition* (CRC Press, Boca Raton FL, 2003)].
- [40] H. J. C. Berendsen, J. P. M. Postma, W. F. van Gunsteren, A. DiNola, and J. R. Haak, *J. Phys. Chem.* **81**, 3684 (1984).
- [41] O. Steinhauser, *Mol. Phys.* **45**, 335 (1982).
- [42] W. Feller, *An Introduction to Probability Theory and Its Applications, Vol. 1, 2nd Edition* (John Wiley & Sons, New York, 1960), pp. 225–226; P. J. Flory, *Statistical Mechanics of Chain Molecules* (John Wiley & Sons, New York, 1969), p. 16.
- [43] In Eq. (13) we normalize the average with the time-dependent number of molecules $n_i(t)$, instead of the total number of cells inside the box as in Ref. [35]. Our choice has the advantage of giving rise to a value of the average dipole in a box \vec{d}_i^v independent of the system density (see for example [44]). However, as a consequence, the distribution of \vec{d}_i^v is not Gaussian, as would be expected by normalizing by a constant factor. We have verified that by using a constant normalization factor we recover a Gaussian distribution. Moreover, we have verified

that our final results are not affected by the choice of the normalization factor in Eq. (13).

- [44] G. Mathias and P. Tavan, *J. Chem. Phys.* **120**, 4393 (2004).
- [45] The definition in Eq. (13) differs from the one introduced in Ref. [35], where the coarse-grained site-dipole field is averaged over spheres with radius R and centered at a distance shorter than $2R$. The definition in Ref. [35] emphasizes the spatial-patterns of coarse-grained site-dipoles, because each molecular dipole contributes to the coarse-grained site-dipole for all the (overlapping) spheres which contain the same molecule. We therefore expect to find patterns that survive for a time shorter than that measured in Ref. [35]. Indeed, we do not find strong evidence of surviving patterns in bulk water within our time resolution.
- [46] At $T = 300$ K we find a autocorrelation time τ_r approximately 10 times smaller than the persistence time found in Ref. [35] for the site-dipoles patterns. This is due to the difference in the definition in Eq. (13). We verify that, by adopting the same definition of Ref. [35], we can reproduce the bulk-water results of Higo et al. See also [45].
- [47] See for example W. Götze, *J. Phys.: Condens. Matter* **11**, A1 (1999); W. Götze and L. Sjogren, *Rep. Prog. Phys.* **55**, 241 (1992); E. Leutheusser, *Phys. Rev. A* **29**, 2765 (1984); W. Götze, in *Liquids, Freezing and the Glass Transition*, Proceedings of the Les Houches Summer School of Theoretical Physics, Session LI, 1989, edited by J. P. Hansen, D. Levesque, and J. Zinn-Justin (North-Holland, Amsterdam, 1991); A. P. Sokolov, J. Hurst, and D. Quitmann, *Phys. Rev. B* **51**, 12 865 (1995).
- [48] R. Schilling and T. Scheidsteiger, *Phys. Rev. E* **56**, 2932 (1997).
- [49] S. Kammerer, W. Kob, and R. Schilling, *Phys. Rev. E* **56**, 5450 (1997).
- [50] T. Franosch, M. Fuchs, W. Götze, M. R. Mayr, and A. P. Singh, *Phys. Rev. E* **56**, 5659 (1997); W. Götze, A. P. Singh, and T. Voigtmann, *Phys. Rev. E* **61**, 6934 (2000); S.-H. Chong and W. Götze, *Phys. Rev. E* **65**, 051201 (2002); *Phys. Rev. E* **65**, 041503 (2002).

TABLE I: Parameters of the fit of $C_1(t)$ in Fig. 1 with Eq. (1). The error on each parameter is $\pm 10\%$.

$T(\text{K})$	A	$\tau_a(\text{ps})$	β
300	0.93	4.9×10^0	0.88
260	0.94	1.7×10^1	0.85
250	0.94	2.8×10^1	0.85
240	0.94	4.9×10^1	0.84
230	0.94	1.1×10^2	0.84
220	0.94	2.7×10^2	0.83
210	0.94	1.1×10^3	0.82

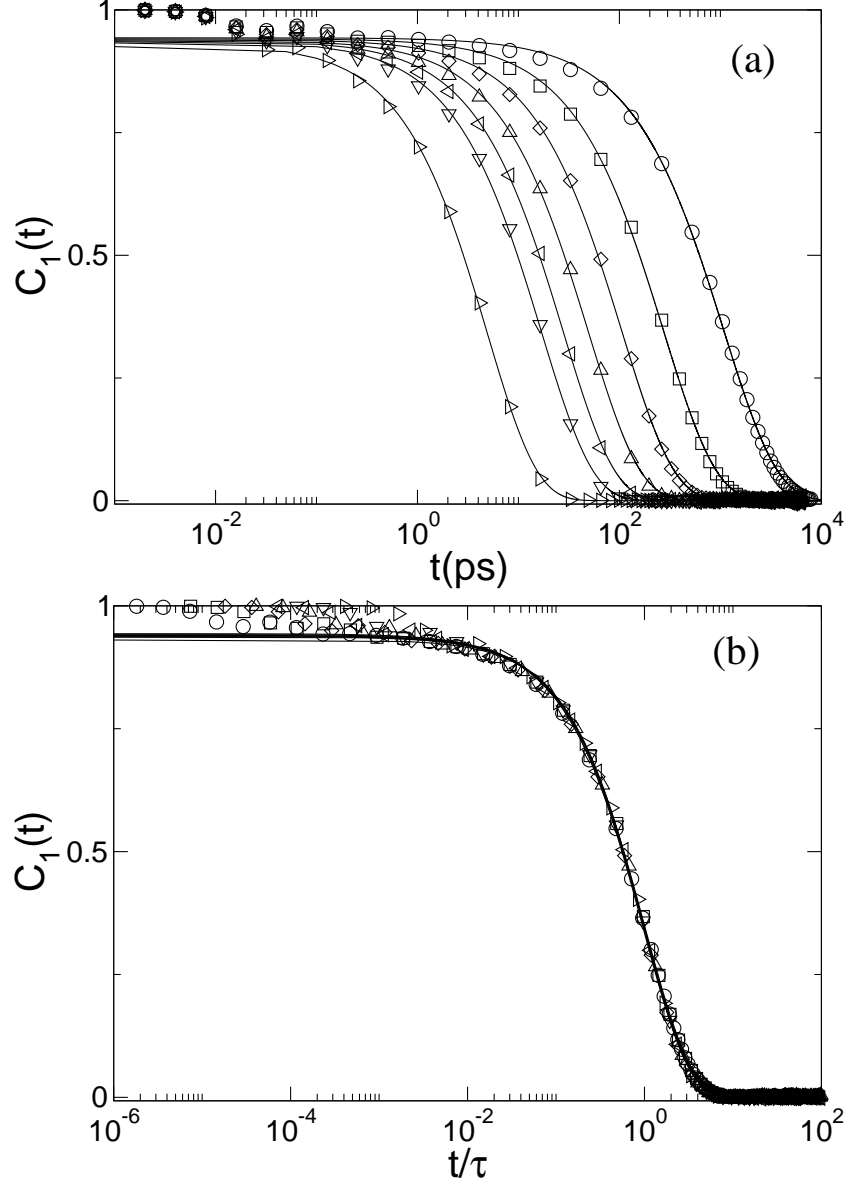


FIG. 1: (a) The orientational autocorrelation function C_1 as a function of time t for $T(K) = 210$ (\circ), 220 (\square), 230 (\diamond), 240 (\triangle), 250 (\triangleleft), 260 (∇), 300(\triangleright). Symbols are simulations, lines are fits over the range for $t \geq 0.03$ ps to Eq. (1) with the fitting parameters listed in Table I. (b) Test of the time-temperature superposition principle, as predicted by MCT. The symbols and the lines for different T fall on a single curve if the times are rescaled by $\tau_a(T)$.

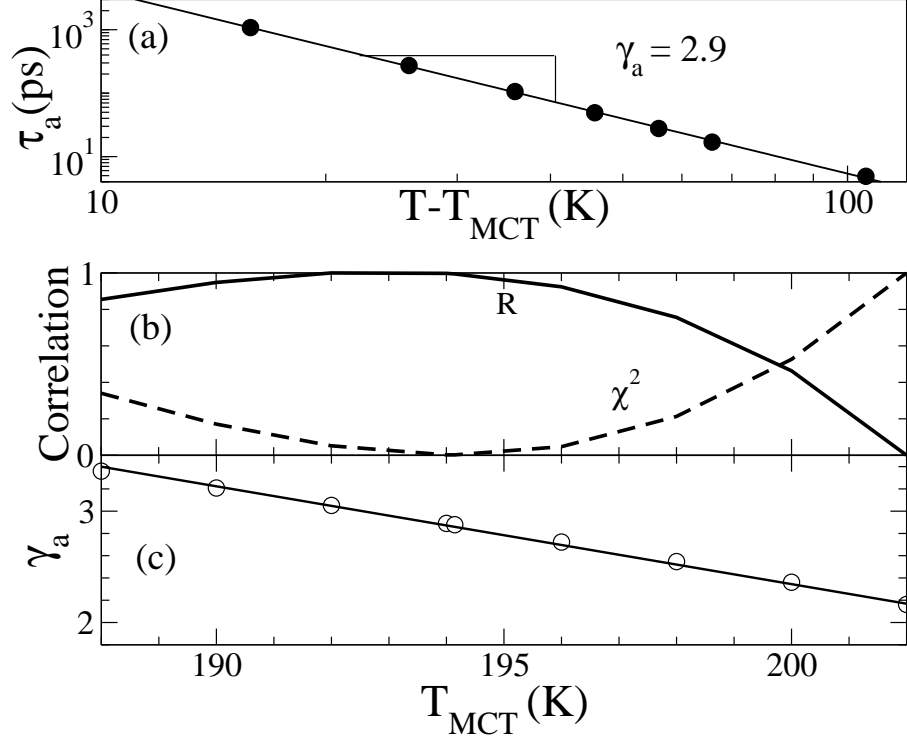


FIG. 2: (a) Power law behavior of orientational autocorrelation time τ_a extracted from $C_1(t)$, as a function of $T - T_{\text{MCT}}$, as predicted by MCT [Eq. (4)]. The line is a fit to the MCT power law with $T_{\text{MCT}} = 194$ K and exponent $\gamma_a = 2.9$. (b) To optimize the fit, we vary T_{MCT} , calculate the autocorrelation coefficient R (solid line) and the χ^2 (dashed line), and choose as our estimate of T_{MCT} the value corresponding to the maximum or minimum of these quantities, within a 10% variation in our range of T . R and χ^2 are rescaled to the maximum and minimum values we found for $188 \text{ K} \leq T_{\text{MCT}} \leq 202 \text{ K}$. (c) The MCT exponent γ_a corresponding to different choices of T_{MCT} . Note that the exponent γ_a decreases almost linearly with increasing choice of T_{MCT} . Based on the results in (b), our estimates are $T_{\text{MCT}} = (194 \pm 4) \text{ K}$ and $\gamma_a = 2.9 \pm 0.3$.

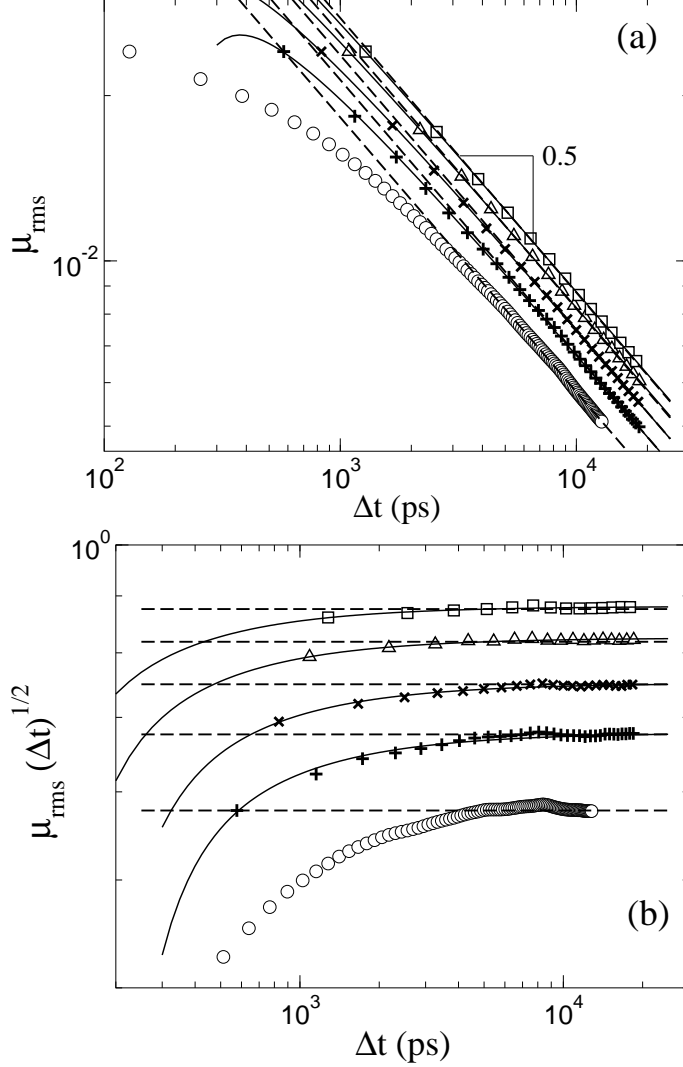


FIG. 3: (a) The μ_{rms} of Eq. (7) for $T = 220$ K, plotted versus Δt for a range of different time steps $\delta t = 128$ ps (\circ), 576 ps ($+$), 832 ps (\times), 1088 ps (\triangle), and 1280 ps (\square). Dashed lines show the predicted asymptotic behavior $\mu_{\text{rms}} \sim 1/\sqrt{\Delta t}$. The fit with Eq. (10) (solid lines) is good when $\delta t \geq 576$ ps, but we are unable to fit the data for $\delta t = 128$ ps, showing that the angle between the dipoles in Eq. (6) is not independent, as assumed in the freely rotating chain model. However, Eq. (10) gives a fair description of the approach to the asymptotic regime. (b) $\mu_{\text{rms}}\sqrt{\Delta t}$ vs Δt approaches a constant asymptotically when $\Delta t \gg \tau_r$. In both panels (a) and (b) the errors are roughly the size of the symbols.

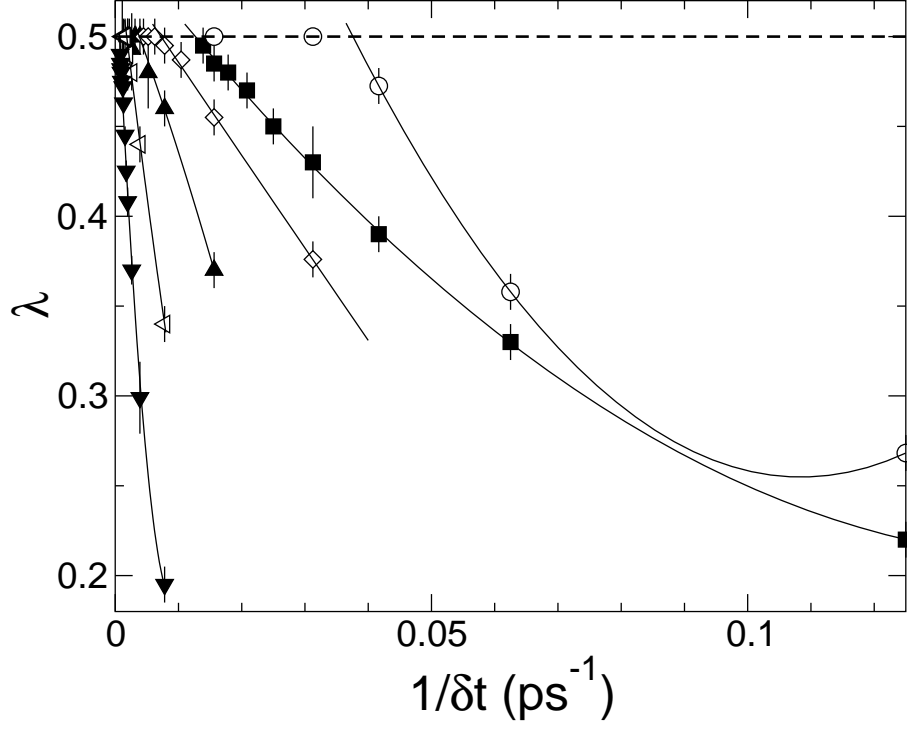


FIG. 4: The exponent λ , defined in Eq. (12) and calculated using the first eight points of the curves in Fig. 3, versus the inverse of time-step δt , for $T = 300$ K (\circ), 260 K (\blacksquare), 250 K (\diamond), 240 K (\blacktriangle), 230 K (\triangleleft), 220 K (\blacktriangledown). Where not shown the errors are smaller than the symbol size. The horizontal dashed line corresponds to $\lambda = 0.5$. By a quadratic fit of the data with $\lambda < 0.5$, we find the self-dipole randomization time τ_r , defined as the value of δt where $\lambda = 1/2$.

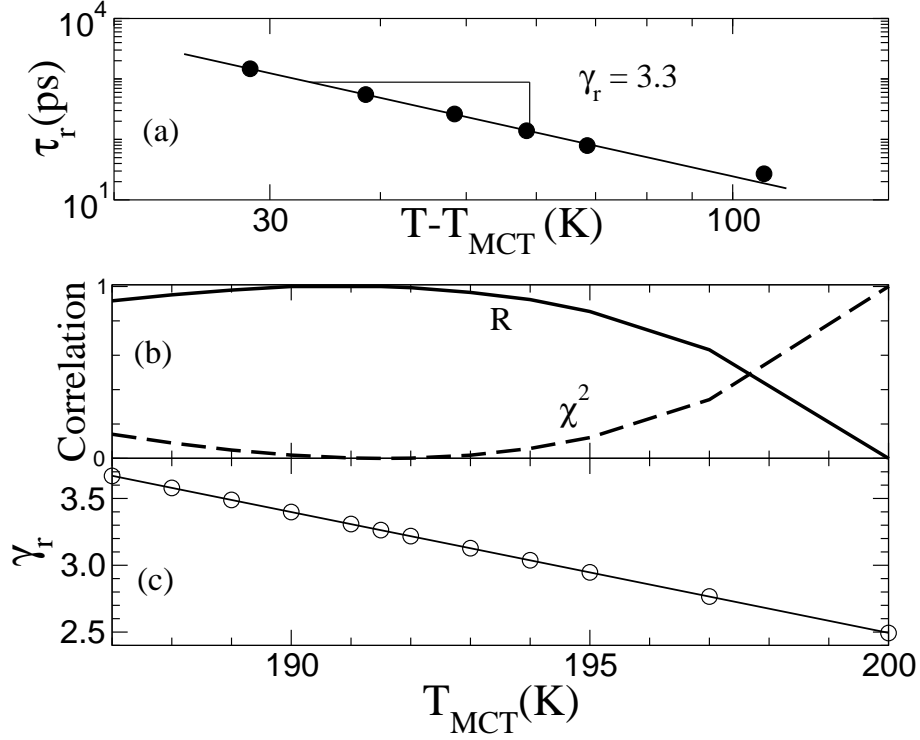


FIG. 5: Analog of Fig. 2 for the self-dipole randomization time τ_r . (a) τ_r follows a power law behavior in $T - T_{\text{MCT}}$ [Eq. (4)], as predicted by MCT. The line is a fit with $T_{\text{MCT}} = 191.5$ K and power $\gamma_r = 3.3$. (b) As in Fig. 2, to optimize the estimate of T_{MCT} we calculate the autocorrelation coefficient R (solid line) and the χ^2 (dashed line). In (b), R and χ^2 are rescaled to the maximum and minimum values we found for $187 \text{ K} \leq T_{\text{MCT}} \leq 200 \text{ K}$. (c) The fitting parameter γ_r corresponding to different estimates of T_{MCT} . The exponent γ_r decreases linearly with increasing estimates of T_{MCT} . Based on the results in (b), our estimates are $T_{\text{MCT}} = (191.5 \pm 2.5) \text{ K}$ and $\gamma_r = 3.3 \pm 0.2$.

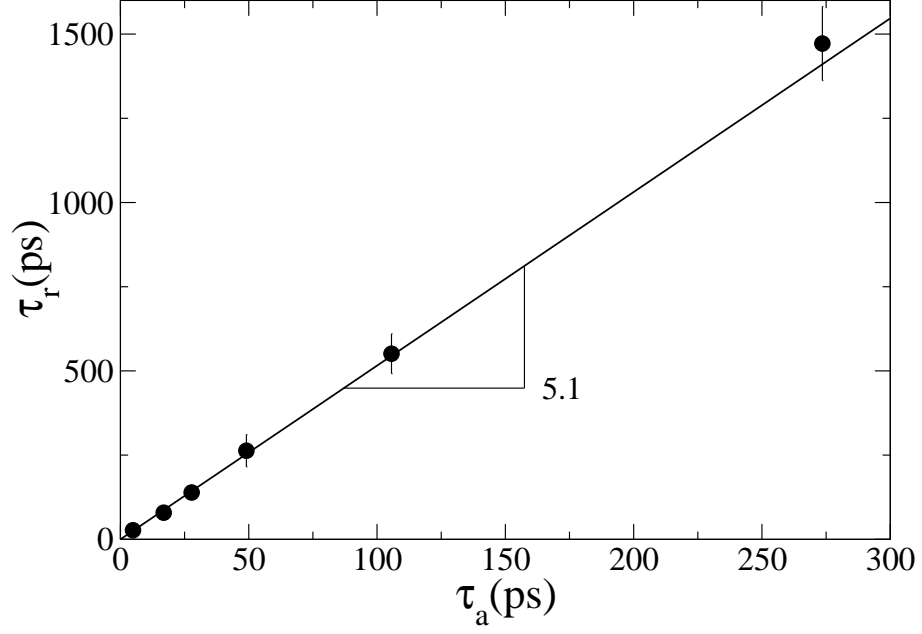


FIG. 6: Parametric plot of the times $\tau_r(T)$ and $\tau_a(T)$, within the range $220 \text{ K} \leq T \leq 300 \text{ K}$, with the lowest time corresponding to the highest T . The line reflects the linear one-parameter fit, $\tau_r = (5.1 \pm 0.2)\tau_a$.

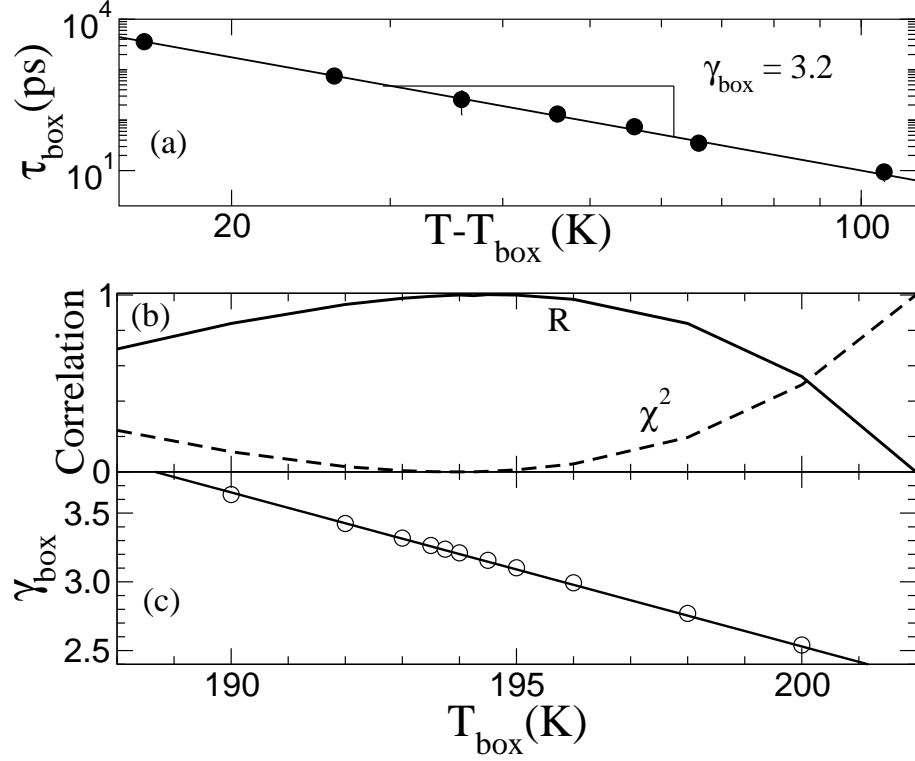


FIG. 7: Analog of Fig. 2 and Fig. 6 for the site-dipole randomization time τ_{box} . (a) We find a power law behavior in $T - T_{\text{box}}$, calculated for $L_{\text{box}} = 3\text{\AA}$. The line is a fit with $T_{\text{MCT}} = 194$ K and exponent $\gamma_{\text{box}} = 3.2$. (b) Optimization analysis for T_{box} : correlation coefficient R (solid line) and χ^2 (dashed line), both rescaled to the maximum and minimum values found for $188 \text{ K} \leq T_{\text{box}} \leq 202 \text{ K}$. (c) The exponent γ_{box} corresponding to different choices of T_{box} , decreases linearly with increasing choice of T_{box} . We estimate $T_{\text{box}} = (194 \pm 2) \text{ K}$ and $\gamma_{\text{box}} = 3.2 \pm 0.2$.

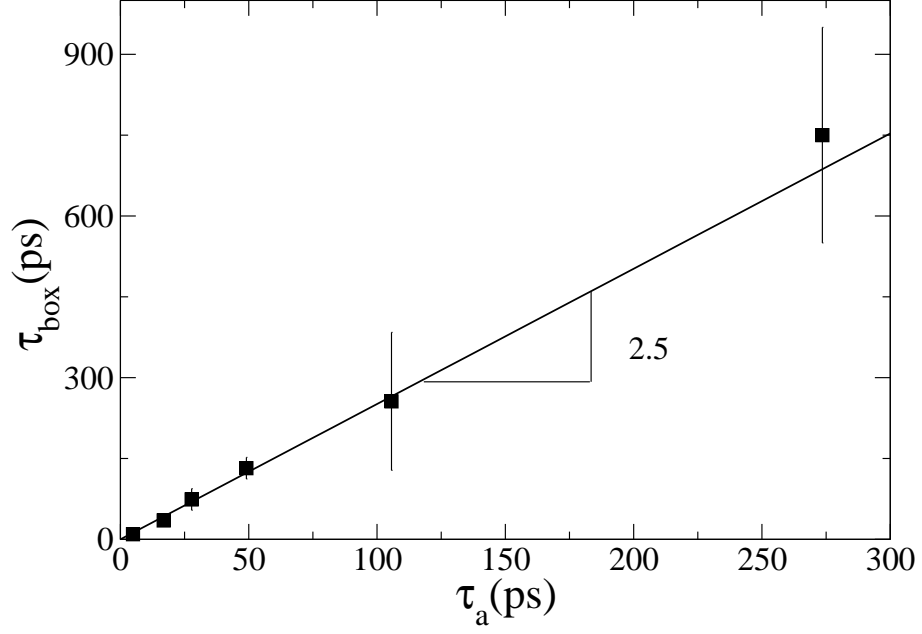


FIG. 8: Analog of Fig. 7: A parametric plot of the site-dipole randomization time $\tau_{\text{box}}(T)$ and the orientational autocorrelation time $\tau_a(T)$ over the range $220 \text{ K} \leq T \leq 300 \text{ K}$, with the lowest time corresponding to the highest T . The line reflects the linear one-parameter fit $\tau_{\text{box}} = (2.5 \pm 0.2)\tau_a$.

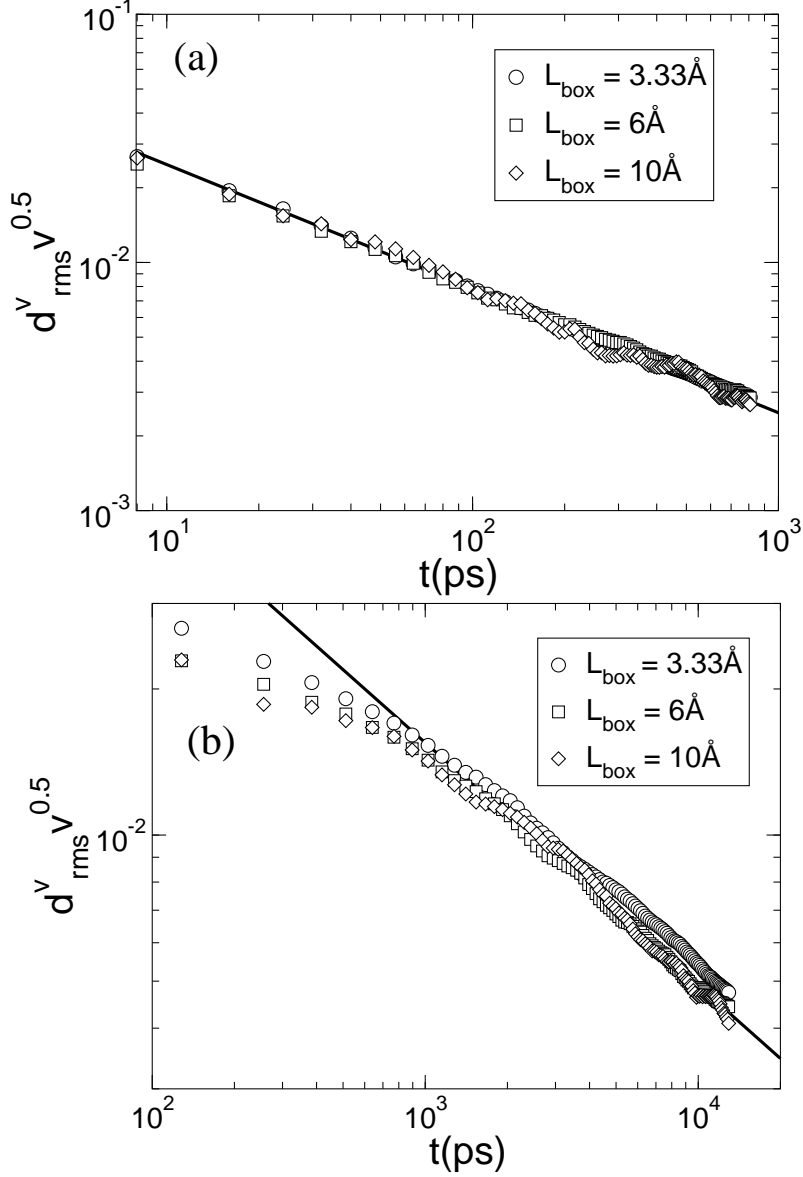


FIG. 9: Size dependence of site-dipole autocorrelation function d_{rms}^v as a function of t for $L_{\text{box}} = 3.33 \text{ \AA}$ (\circ), 6 \AA (\square), 10 \AA (\diamond) and for two different temperatures (a) $T = 300$ K and (b) $T = 220$ K. In (a) the line is a fit of data for $L_{\text{box}} = 3.33 \text{ \AA}$ with $d_{\text{rms}}^v = a/\sqrt{t}$, with $a = 0.08 \pm 0.01$. In (b) the same fit is for the data at $L_{\text{box}} = 6 \text{ \AA}$ and $t > 10^2$, with $a = 0.49 \pm 0.01$. For each T all the values of $d_{\text{rms}}^v \sqrt{v}$ overlap, suggesting that the orientational autocorrelation is short-range.

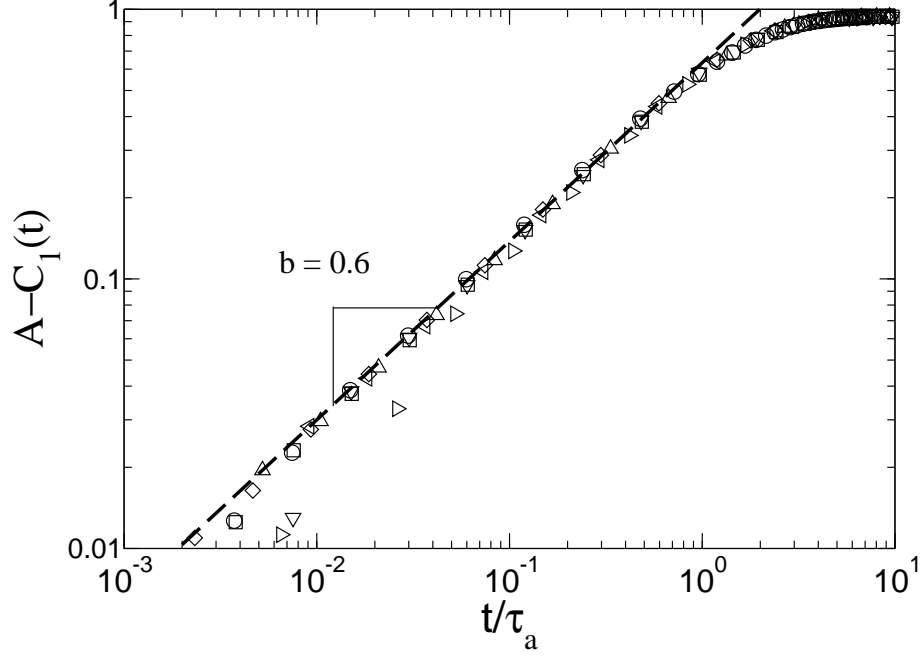


FIG. 10: Test of the von Schweidler law, Eq. (A1). It is well verified roughly over two decades, for $T \leq 250$ K. Data for higher T depart from this law at short times. Symbols are as in Fig. 1. Dashed line is the fit to Eq. (A1) of the data for $T = 230$ K over the fitting range $0.01 \leq A - C_1 \leq 0.50$ with the result $b = 0.6 \pm 0.1$.